



Model Order Reduction Strategies for the Computation of Compact Machine Tool Models

Quirin Aumann¹, Peter Benner^{1,2}, Jens Saak^{1,2}, and Julia Vettermann¹(✉)

¹ Chemnitz University of Technology,
Reichenhainer Str. 41, 09126 Chemnitz, Germany
julia.vettermann@mathematik.tu-chemnitz.de

² Max Planck Institute for Dynamics of Complex Technical Systems,
Sandtorstr. 1, 39106 Magdeburg, Germany

Abstract. The deviation of the tool center point (TCP) of a machine tool from its desired location needs to be assessed correctly to ensure an accurate and safe operation of the machine. A major source of TCP deviation are thermal loads, which are constantly changing during operation. Numerical simulation models help predicting these loads, but are typically large and expensive to solve. Especially in (real-time feedback) control settings, but also to ensure an efficient design phase of machine tools, it is inevitable to use compact reduced-order surrogate models which approximate the behavior of the original system but are much less computationally expensive to evaluate. Model order reduction (MOR) methods generate computationally efficient surrogates. Classic intrusive methods require explicit access to the assembled system matrices. However, commercial software packages, which are typically used for the design of machine tools, do not always allow an unrestricted access to the required matrices. Non-intrusive data-driven methods compute surrogates requiring only input and output data of a dynamical system and are therefore independent of the discretization method. We evaluate the performance of such data-driven approaches to compute cheap-to-evaluate surrogate models of machine tools and compare their efficacy to intrusive MOR strategies. A focus is put on modeling the machine tool via individual substructures, which can be reduced independently of each other.

Keywords: Model order reduction · Loewner framework · Balanced truncation · Rational interpolation · Machine tools

1 Introduction

Model order reduction (MOR) plays an important role in the energy efficient correction of thermally induced errors of machine tools during the production process [10, 18]. Therefore, compact simulation models for fast computations are required for the efficient operation of machine tools enabling, e.g., online correction of the thermally induced displacement of the tool center point (TCP), predictive maintenance, or online parameter estimation. Such models are also an enabler-technology for digital twins of machine tools [12].

Machine tools are complex technical systems consisting of a number of interconnected machine components, which can move relative to each other. In the following, these components will be referred to as subassemblies. The thermal behavior of the machine and its subassemblies is often modeled using the finite element method (FEM). Due to the need to resolve also small geometrical features of the machine tool, the number of degrees of freedom in such numerical models is typically high, and methods to reduce the computational complexity of solving the associated systems of equations are required. System-theoretic MOR methods have proven to be able to reduce these computational costs by computing surrogate models approximating the input/output behavior of the original model but having a much smaller size [2]. These methods have also been successfully applied to machine tool models [11, 14, 18]. They often show a better performance compared to modal methods [5, 16], which are not recommended for the reduction of thermal problems [4, 8].

An alternative to system-theoretic or modal methods are data-driven procedures. They construct surrogate models approximating the input/output behavior of the original model using snapshot data, e.g., evaluations of its transfer function. Data-driven methods can also be referred to as non-intrusive methods, because unlike intrusive system-theoretic or modal MOR methods, they do not require access to the matrices describing the numerical model. Especially when closed-source or proprietary finite element software solutions are employed, as it is often the case in industrial applications, these matrices are difficult or inconvenient to obtain and intrusive MOR methods might not always fit the design workflow of machine tools. However, the snapshot data required for data-driven MOR methods can be obtained from standard finite element software by performing, e.g., a frequency sweep analysis.

An efficient modeling of the time-varying coupling conditions between subassemblies is crucial for a successful simulation of different work processes. Using an approach originally presented by Hernández-Becerro et al. [11], it is possible to precompute parts of the coupling terms required to model the thermal flow between subassemblies. Depending on the position of the coupling at the current simulation time, the coupling condition can be assembled by a linear combination of the precomputed values. As no further modifications of the numerical model are required, the same numerical model can be used to model any relative movements between subassemblies. The precomputed coupling terms can be added as additional inputs and outputs to the original system description, such that the coupling can also be realized in the reduced space.

In this contribution, we show how a data-driven MOR strategy based on the Loewner framework [15] can be used to obtain reduced-order models of machine tool systems consisting of multiple subassemblies. Surrogate models computed by the Loewner framework can be expressed as state space systems. Therefore they can easily be integrated into existing modeling workflows. We also evaluate the impact of the high number of system inputs and outputs added by the coupling conditions on the approximation quality and reduction efficacy. The performance of the resulting surrogate models is compared to reduced-order models computed

using balanced truncation, an intrusive MOR method. Balanced truncation is especially suited for the reduction of thermal problems as it shows a global error behavior and an a priori error bound can be computed efficiently [1].

This contribution is structured as follows: In Sect. 2 we show some modeling aspects of machine tools. In Sect. 3 we discuss suitable intrusive and non-intrusive MOR techniques. Numerical investigations including a comparison of different reduction methods for a simplified 3-axis machine tool model are described in Sect. 4. A summary of our findings in Sect. 5 concludes the contribution.

2 Modeling of Machine Tools

The thermal behavior of a body of homogeneous and temporally constant material can be expressed by a partial differential equation (PDE) for the temperature field $T(t, \delta)$ at time t and location δ as

$$\rho c_p \frac{\partial}{\partial t} T(t, \delta) - \Delta \lambda T(t, \delta) = \dot{q}(t, \delta). \quad (1)$$

The external thermal load is given by \dot{q} and the material is characterized by its density ρ , heat capacity c_p , and conductivity λ . The dot defines a derivative in time and $\Delta = \nabla \cdot \nabla$ is the Laplace operator.

2.1 System-Theoretic Approach

Discretizing this PDE in space with, e.g., the finite element method allows to formulate the system in a state-space representation

$$\Sigma: \begin{cases} \mathbf{E}\dot{\mathbf{x}}(t) = \mathbf{A}\mathbf{x} + \mathbf{B}\mathbf{u}(t), \\ \mathbf{y}(t) = \mathbf{C}\mathbf{x}, \end{cases} \quad (2)$$

with capacity and conductivity matrices $\mathbf{E}, \mathbf{A} \in \mathbb{R}^{n \times n}$, input and output mappings $\mathbf{B} \in \mathbb{R}^{n \times m}$, $\mathbf{C} \in \mathbb{R}^{p \times n}$, states $\mathbf{x} \in \mathbb{R}^n$, inputs $\mathbf{u} \in \mathbb{R}^m$, and outputs $\mathbf{y} \in \mathbb{R}^p$. Many MOR methods require the original system to be described in frequency domain. This transformation is performed using the Laplace transform and setting the Laplace constant to $s = i\omega$, where ω is the excitation frequency. An important analysis tool of frequency domain systems is the transfer function, which depicts the input to output mapping of the system. For a thermal system in state-space form (2), the transfer function is given by

$$\mathbf{H}(s) = \mathbf{C}(s\mathbf{E} - \mathbf{A})^{-1}\mathbf{B}. \quad (3)$$

2.2 Efficient Modeling of Time-Varying Thermal Couplings

Machine tools are composed of different subassemblies which can move relative to each other. This results in time-varying coupling conditions between the subassemblies, which have to be represented efficiently in the modeling process,

as a re-meshing of the complete model after each relative movement is not feasible. Another benefit of modeling the subassemblies independent of each other is that individual parts can be exchanged during the design process without affecting the other parts of the machine.

In the following, the heat transfer between machine subassemblies is modeled with bushing interface conditions, a type of multi point constraint. Here, the heat flux \dot{q} between two coupled boundaries is defined by relating the average temperature at the boundaries $\bar{\theta}_1, \bar{\theta}_2$ and scaling it with the heat transfer coefficient h :

$$\dot{q} = h (\bar{\theta}_1 - \bar{\theta}_2). \quad (4)$$

The benefit of this approach is that it is independent of the discretization of the boundaries and that no matching grids are required. It should be noted that bushing interface conditions are not accurate for interfaces with high temperature gradients due to the averaging performed in (4). Many coupling interfaces in machine tool models, for example the interaction between a rail and a carriage, are relatively small and have a rather uniform temperature distribution, so bushing conditions can be applied efficiently in this setting [10].

In order to realize an efficient time-varying thermal coupling of the subassemblies, we use an approach by Hernández-Becerro et al. [11]. This strategy precomputes general boundary terms, which are valid for any relative position of the two subassemblies, and makes a re-evaluation of the coupling terms for changing positions unnecessary. The moving interface is defined by a weighting function $w(d, d_c)$ on the boundaries with the location of the respective mesh node on the boundary d and the center position of the interface d_c . An interaction between the boundaries only happens for $w(d, d_c) \neq 0$. The gist of the approach is to separate the variables d and d_c , such that all contributions depending on d can be precomputed. This is done by approximating the weighting function by a Fourier series

$$w(d, d_c) = a_0 + \sum_{k=1}^{n_h} a_k(d_c) \cos(2\pi kd) + \sum_{k=1}^{n_h} b_k(d_c) \sin(2\pi kd),$$

and precomputing the terms which are not depending on d_c for all nodes on the boundary. In practice, this can be achieved by applying corresponding loads on the boundary. A vector \mathbf{b} defining the weighted average over the corresponding boundary, given the location of the coupling d_c , can then be formed by a linear combination of the precomputed vector quantities and some scalar factors:

$$\mathbf{b}(d_c) = \mathbf{b}_0 + \sum_{k=1}^{n_h} a_k(d_c) \mathbf{b}_{k,\cos} + \sum_{k=1}^{n_h} b_k(d_c) \mathbf{b}_{k,\sin}.$$

This vector \mathbf{b} acts as input and output in the system-theoretic formulation of the thermal system (2), as, on the one hand, it averages the temperature on the boundary according to the weighting function, on the other hand, it maps the resulting heat flux from (4) back onto the boundary.

3 Model Order Reduction for Machine Tools

The computational cost for evaluating numerical models of machine tools (2) and (3) is often very high and thus may hinder an efficient design phase and prohibit their direct use for online control. A large part of the computational complexity roots in the need for (repeated) decompositions of matrices of order n , which is the number of degrees of freedom of the model. In practical applications, n can be very large, as also complex geometric features need to be resolved by a fine mesh. MOR methods find a surrogate model

$$\widehat{\Sigma}: \begin{cases} \widehat{\mathbf{E}}\dot{\widehat{\mathbf{x}}}(t) = \widehat{\mathbf{A}}\widehat{\mathbf{x}} + \widehat{\mathbf{B}}\mathbf{u}(t), \\ \widehat{\mathbf{y}}(t) = \widehat{\mathbf{C}}\widehat{\mathbf{x}}, \end{cases} \quad (5)$$

with the reduced matrices $\widehat{\mathbf{E}}, \widehat{\mathbf{A}} \in \mathbb{R}^{r \times r}$, $\widehat{\mathbf{B}} \in \mathbb{R}^{r \times m}$, $\widehat{\mathbf{C}} \in \mathbb{R}^{p \times r}$ and the states in reduced space $\widehat{\mathbf{x}} \in \mathbb{R}^r$. The model (5) can serve as a surrogate for the original model (2), if the reduced-order model's output is up to a specific tolerance ε similar to the original output, i.e.

$$\|\mathbf{y} - \widehat{\mathbf{y}}\| \leq \varepsilon \|\mathbf{u}\|,$$

under an appropriate norm $\|\cdot\|$ and for all feasible inputs \mathbf{u} . The transfer function of the reduced-order model is given by

$$\widehat{\mathbf{H}}(s) = \widehat{\mathbf{C}} \left(s\widehat{\mathbf{E}} - \widehat{\mathbf{A}} \right)^{-1} \widehat{\mathbf{B}}. \quad (6)$$

The underlying reduced-order model is an appropriate surrogate, if

$$\left\| \mathbf{H} - \widehat{\mathbf{H}} \right\| \leq \varepsilon,$$

as for appropriately chosen norms,

$$\|\mathbf{y} - \widehat{\mathbf{y}}\| \leq \left\| \mathbf{H} - \widehat{\mathbf{H}} \right\| \cdot \|\mathbf{u}\|.$$

Among other methods, the reduced quantities in (5) and (6) can be obtained from projecting the original system matrices onto a lower dimensional subspace, which contains the sought after solution [2]. This subspace $\mathcal{V} \subset \mathbb{C}^n$ and the corresponding test space $\mathcal{W} \subset \mathbb{C}^n$ are spanned by two truncation matrices $\mathbf{V}, \mathbf{W} \in \mathbb{C}^{n \times r}$, respectively. The reduced-order quantities can then be computed by

$$\widehat{\mathbf{E}} = \mathbf{W}^H \mathbf{E} \mathbf{V}, \quad \widehat{\mathbf{A}} = \mathbf{W}^H \mathbf{A} \mathbf{V}, \quad \widehat{\mathbf{B}} = \mathbf{W}^H \mathbf{B}, \quad \widehat{\mathbf{C}} = \mathbf{C} \mathbf{V}. \quad (7)$$

Note, that it is often convenient to choose real-valued truncation matrices \mathbf{V}, \mathbf{W} to preserve the realness of the original model also in reduced space.

3.1 Intrusive MOR with Balanced Truncation

Balanced truncation (BT) is a widely used projection-based MOR method. Balancing in this context means to transform the system to a form where reachability and observability of the system states are equivalent concepts. This transformation does not influence the input/output behavior, as it leads to a different realization of the same system. States which are at the same time hard to reach and yield little observation energy can be identified given such representation. Truncating these states reduces the size of the system while the input/output behavior is not greatly influenced. Balanced truncation also offers a computable a priori error bound relating the energy of the truncated states to the approximation error of the surrogate model [1]. The truncation matrices \mathbf{V} , \mathbf{W} for (7) are computed by performing a singular value decomposition (SVD) of the system Gramians and truncating all singular vectors whose corresponding singular values do not contribute considerably to the truncation error. Solving the dual Lyapunov equations

$$\begin{aligned} \mathbf{A}\mathbf{P}\mathbf{E}^\top + \mathbf{E}\mathbf{P}\mathbf{A}^\top + \mathbf{B}\mathbf{B}^\top &= 0 \\ \mathbf{A}^\top\mathbf{Q}\mathbf{E} + \mathbf{E}^\top\mathbf{Q}\mathbf{A} + \mathbf{C}^\top\mathbf{C} &= 0 \end{aligned} \quad (8)$$

yields the required reachability Gramian \mathbf{P} and observability Gramian $\mathbf{E}^\top\mathbf{Q}\mathbf{E}$. The system matrices in (8) are often large and sparse. In this case, there is a variety of established and efficient solution algorithms, which compute low-rank approximations of the Gramians, such that $\mathbf{P} \approx \mathbf{Z}_P\mathbf{Z}_P^\top$ and $\mathbf{E}^\top\mathbf{Q}\mathbf{E} \approx \mathbf{Z}_Q\mathbf{Z}_Q^\top$; see, e.g., [6]. If the states corresponding to the r largest singular values $\Sigma_1 = \text{diag}(\sigma_1, \dots, \sigma_r)$ of the SVD

$$\mathbf{S}\Sigma\mathbf{T} = [\mathbf{S}_1\mathbf{S}_2] \begin{bmatrix} \Sigma_1 \\ \Sigma_2 \end{bmatrix} [\mathbf{T}_1\mathbf{T}_2]^\top = \mathbf{Z}_Q^\top\mathbf{Z}_P$$

should be preserved in the reduced-order model, the corresponding truncation matrices are formed from the left and right singular vectors as

$$\mathbf{V} = \mathbf{Z}_P\mathbf{T}_1\Sigma_1^{-\frac{1}{2}}, \quad \mathbf{W} = \mathbf{Z}_Q\mathbf{S}_1\Sigma_1^{-\frac{1}{2}}.$$

Balanced truncation preserves the stability of the original system automatically.

3.2 Non-intrusive MOR with the Loewner Framework

The computation of system Gramians or their low-rank factors requires direct access to the original system matrices. However, these matrices are often not readily available or inconvenient to obtain explicitly. The Loewner framework [15] uses solely transfer function measurements or evaluations to find a surrogate model, which interpolates the transfer function of the original system (3), and provides a realization of this interpolant as a state-space system. The general procedure is shortly summarized in the following.

Given N measurements $\mathbf{H}_k \in \mathbb{C}^{p \times m}$, $k = 1, \dots, N$ of the transfer function at some locations $s_k \in \mathbb{C}$, the data is partitioned into two disjoint sets

$$\begin{cases} (\lambda_i, \mathbf{r}_i, \mathbf{w}_i), \text{ where } \lambda_i = s_i, \mathbf{w}_i = \mathbf{H}_i \mathbf{r}_i, i = \{1, \dots, \rho\}, \\ (\mu_j, \mathbf{l}_j, \mathbf{v}_j), \text{ where } \mu_j = s_{\rho+j}, \mathbf{v}_j^H = \mathbf{l}_j^H \mathbf{H}_{\rho+j}, j = \{1, \dots, \nu\}, \end{cases}$$

with $N = \rho + \nu$ and right and left tangential directions $\mathbf{r}_i, \mathbf{l}_j$. For numerical reasons it is often beneficial to partition the data in an alternating way. The partitioned data is now arranged in the Loewner and shifted Loewner matrices \mathbb{L} and \mathbb{L}_σ given by

$$\mathbb{L} = \begin{bmatrix} \frac{\mathbf{v}_1 \mathbf{r}_1 - \mathbf{l}_1 \mathbf{w}_1}{\mu_1 - \lambda_1} & \dots & \frac{\mathbf{v}_1 \mathbf{r}_\rho - \mathbf{l}_1 \mathbf{w}_\rho}{\mu_1 - \lambda_\rho} \\ \vdots & \ddots & \vdots \\ \frac{\mathbf{v}_\nu \mathbf{r}_1 - \mathbf{l}_\nu \mathbf{w}_1}{\mu_\nu - \lambda_1} & \dots & \frac{\mathbf{v}_\nu \mathbf{r}_\rho - \mathbf{l}_\nu \mathbf{w}_\rho}{\mu_\nu - \lambda_\rho} \end{bmatrix},$$

$$\mathbb{L}_\sigma = \begin{bmatrix} \frac{\mu_1 \mathbf{v}_1 \mathbf{r}_1 - \lambda_1 \mathbf{l}_1 \mathbf{w}_1}{\mu_1 - \lambda_1} & \dots & \frac{\mu_1 \mathbf{v}_1 \mathbf{r}_\rho - \lambda_\rho \mathbf{l}_1 \mathbf{w}_\rho}{\mu_1 - \lambda_\rho} \\ \vdots & \ddots & \vdots \\ \frac{\mu_\nu \mathbf{v}_\nu \mathbf{r}_1 - \lambda_1 \mathbf{l}_\nu \mathbf{w}_1}{\mu_\nu - \lambda_1} & \dots & \frac{\mu_\nu \mathbf{v}_\nu \mathbf{r}_\rho - \lambda_\rho \mathbf{l}_\nu \mathbf{w}_\rho}{\mu_\nu - \lambda_\rho} \end{bmatrix}.$$

If the matrix pencil $(\mathbb{L}_\sigma, \mathbb{L})$ is regular, $\mathbf{H}_r(z) = \mathbf{Y} (\mathbb{L}_\sigma - z\mathbb{L})^{-1} \mathbf{X}$ tangentially interpolates the given data, such that $\mathbf{H}_r(\lambda_i) \mathbf{r}_i = \mathbf{w}_i$, $\mathbf{l}_j^H \mathbf{H}_r(\mu_j) = \mathbf{v}_j^H$. A state space realization of the surrogate is thus given by

$$\begin{aligned} \mathbf{E}_\mathbb{L} &= -\mathbb{L}, \quad \mathbf{A}_\mathbb{L} = -\mathbb{L}_\sigma, \\ \mathbf{B}_\mathbb{L} &= \mathbf{X} = [\mathbf{v}_1^H, \dots, \mathbf{v}_\nu^H]^H, \quad \mathbf{C}_\mathbb{L} = \mathbf{Y} = [\mathbf{w}_1, \dots, \mathbf{w}_\rho]. \end{aligned} \tag{9}$$

The dimension of this system can further be reduced by projection. The required truncation matrices \mathbf{V}, \mathbf{W} are concatenations of the right and left singular vectors obtained from an SVD of \mathbb{L} . Truncating the matrices of singular vectors after r columns and projecting the Loewner realization (9) using (7) yields a reduced-order model of order r . Note, that it is also possible to use uncompressed transfer function data, i.e. omitting the tangential directions. This results in Loewner matrices with a block structure, as every transfer function evaluation has dimension $p \times m$. However, if the system that shall be approximated has a high number of inputs and outputs, the Loewner matrices grow fast. In such cases the resulting surrogate may be either too large for an efficient use or the SVD may be not computationally feasible anymore. Therefore, the compression of the original via tangential directions is often a more efficient approach, although it involves a loss of information for the reduced-order model. Other interpolation-based MOR methods employ similar strategies [1].

As the resulting surrogates should be used in time domain, they have to preserve the realness and stability of the original model. Realness can be enforced

in the Loewner framework by adding also the complex conjugates of the transfer function measurements to the database. In practice, this is performed by pre- and post-multiplying the Loewner and shifted Loewner matrices by block-diagonal matrices

$$\mathbf{J} = \mathbf{I} \otimes \left(\frac{1}{\sqrt{2}} \begin{bmatrix} 1 & -i \\ 1 & i \end{bmatrix} \right),$$

where \mathbf{I} is an identity matrix of appropriate size. \mathbf{X} , \mathbf{Y} in (9) have to be modified accordingly [3].

Realizations computed with the Loewner framework do not automatically preserve the stability of the original model, so the surrogate computed with the Loewner framework has to be post-processed. Different strategies for ensuring the stability of the Loewner surrogate can be identified: (i) truncating the unstable part of the model, (ii) flipping the unstable part, or (iii) computing a stable approximation to the original interpolant that is optimal regarding an appropriate norm [9,13]. In the following, we will use the first strategy and truncate all states of the identified system (9) which correspond to unstable eigenvalues, i.e. eigenvalues with a positive real part. For this, the unstable and infinite parts of the system need to be identified. This can be achieved by finding transformation matrices \mathbf{T}_L , \mathbf{T}_R , such that

$$\mathbf{T}_L (\lambda \mathbf{E}_L - \mathbf{A}_L) \mathbf{T}_R = \lambda \begin{bmatrix} \mathbf{E}_s & & \\ & \mathbf{E}_u & \\ & & \mathbf{E}_\infty \end{bmatrix} - \begin{bmatrix} \mathbf{A}_s & & \\ & \mathbf{A}_u & \\ & & \mathbf{A}_\infty \end{bmatrix}.$$

Here, subscript \cdot_s stands for the stable, \cdot_u for the unstable, and \cdot_∞ for the infinite part of the system. In practice, such transformation can be achieved with the help of the matrix disk and sign functions; see, e.g., [7]. Using the ingredients summarized above, it is possible to compute real and stable realizations of systems, from which only transfer function data are available.

4 Numerical Experiments

For the following numerical experiments, we consider a model of a general 3-axis machine tool. The machine consists of four subassemblies: the machine bed and three sliders for independent movements in x , y , and z -direction. The geometry has been described in [17]; a sketch of the geometry is given in Fig. 1. The differential equation for the temperature field acting on the machine (1) is discretized with a finite element method using the MATLAB Partial Differential Equation Toolbox. As only a movement in y -direction is modeled in the following experiments, two subassemblies are formed: one consisting of the machine bed and the x -slider, referred to as **A1** in the following, and **A2** consisting of the sliders for the y and z -directions. The guide rail along which **A2** is moving measures 1400 mm. The resulting numerical models have orders of $n_{A1} = 22\,799$ and $n_{A2} = 18\,685$, respectively. The system is subject to two external heat fluxes, one at the TCP location and one at the top of the workpiece. Additionally, we apply

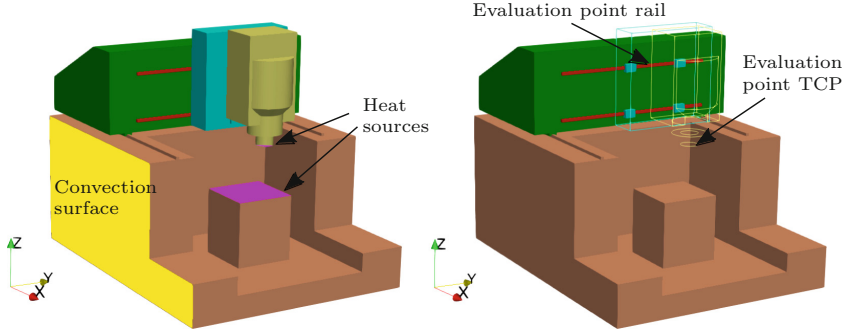


Fig. 1. Left: Sketch of the 3-axis machine tool model consisting of machine bed (brown) and three sliders (x -direction: dark green; y -direction: cyan; z -direction: yellow). The guide rail for the y -slider is marked in red. Right: Subassembly A2 is visualized as wire frame. The guide cars attached to A2 and moving along the guide rail are drawn solid and marked in cyan.

heat fluxes at the guide cars of A2 to model heat resulting from friction (cf. Fig. 1). Exchange of heat between the subassemblies due to radiation is neglected. Energy is dissipated by convection boundary conditions applied to the outer walls of the machine bed.

The subassemblies are coupled via four guide cars, two moving along the upper and lower rail of A1 each. This coupling is realized with the method described in Sect. 2.2 and adds 44 inputs and outputs to A1, respectively 4 inputs and outputs to A2. Only one input/output per location is required for A2, as the coupling location only moves along the rail and is stationary at the coupling points on the y -slider. These additional inputs and outputs are equivalent in original space. However, this is not the case in reduced space, as often $\mathbf{V} \neq \mathbf{W}$. Therefore it is important to use the reduced outputs $\hat{\mathbf{C}} = \mathbf{C}\mathbf{V}$ to obtain the average temperatures θ_1, θ_2 in (4) and the reduced inputs $\hat{\mathbf{B}} = \mathbf{W}^H\mathbf{B}$ to apply the resulting load \dot{q} to the interface. The slider moves for 600 s with constant velocity along the guide in y -direction and changes direction when one end of the rail is reached. After this time, the machine stops and enters a cooling phase. Here, the external heat flux is set to zero. The movement profile of subassembly A2 is given in Fig. 2. We evaluate the temperature at the TCP and at a point located in the middle of the upper rail of A1 during the complete work process.

Surrogate models for an efficient time simulation of the work process are computed using balanced truncation and the Loewner framework as described in Sect. 3. For the Loewner framework, we first compute samples of the transfer function at 200 logarithmically distributed frequencies between $\omega = [1 \cdot 10^{-6}, 1 \cdot 10^{-2}] \text{ rad s}^{-1}$ for both subassemblies. The main dynamics of both systems can be observed in this frequency range and the sampling rate ensures a sufficiently high resolution to capture all important features of the transfer functions. The samples are post-processed to obtain real-valued Loewner and shifted Loewner matrices as described in Sect. 3.2. Their normalized singular

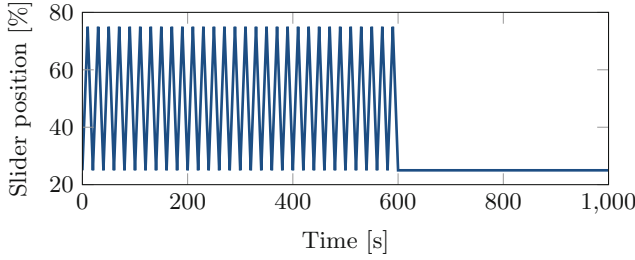


Fig. 2. Movement of subassembly A2 along the rails on A1. The position of the midpoint of A2 is plotted in relation to the total length of the rail.

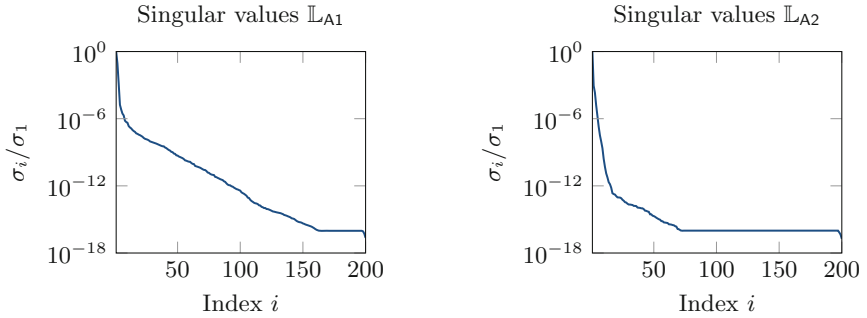


Fig. 3. Singular values of the Loewner matrices \mathbb{L} for A1 (left) and A2 (right).

values are given in Fig. 3 and show a rapid decay for A2, but a slower decay for A1. This means that a larger reduced-order model is required to approximate A1 accurately. The reason for this is the higher number of inputs and outputs of A1 compared to A2.

We truncate all states of the surrogate model which correspond to singular values $\sigma_i < 1 \cdot 10^{-12}$ and remove unstable poles. This leads to stable and real-valued surrogates with order $r_{A1} = 92$ and $r_{A2} = 14$, respectively. The sizes of the reduced-order models computed from balanced truncation are set to the same values to allow a fair comparison. The time simulation results for both surrogate models as well as the reference solution obtained from the full-order model and the corresponding errors relative to the solution of the full-order model are given in Figs. 4 and 5. At the TCP the temperature rises smoothly, as a constant heat flux is applied here until $t = 600$ s. After this, the machine cools slowly. The effect of the moving interface is clearly visible in Fig. 5, where the temperature at the midpoint of the upper rail in the subassembly A1 is evaluated. As the heat sources are located on the guide cars on A2, which are constantly moving along the rail, the increase in temperature is oscillating, depending on where the cars are located. Both surrogates approximate the full order model with acceptable errors. It should be noted that also the dynamic behavior of the moving interface can be approximated well by the reduced-order models.

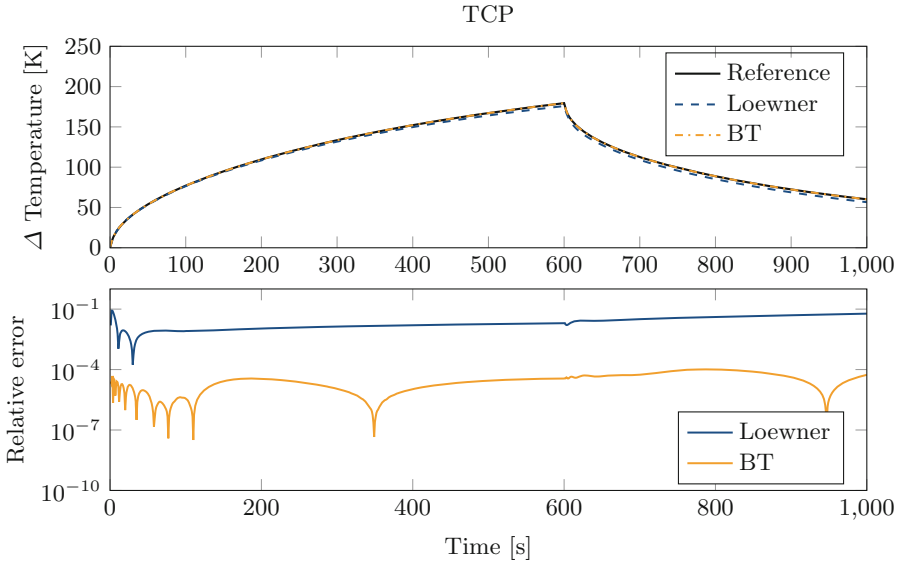


Fig. 4. Temperature change at TCP during the simulated work process. Time responses of the reference full order model and the surrogate models computed by the Loewner framework and balanced truncation as well as the corresponding relative errors.

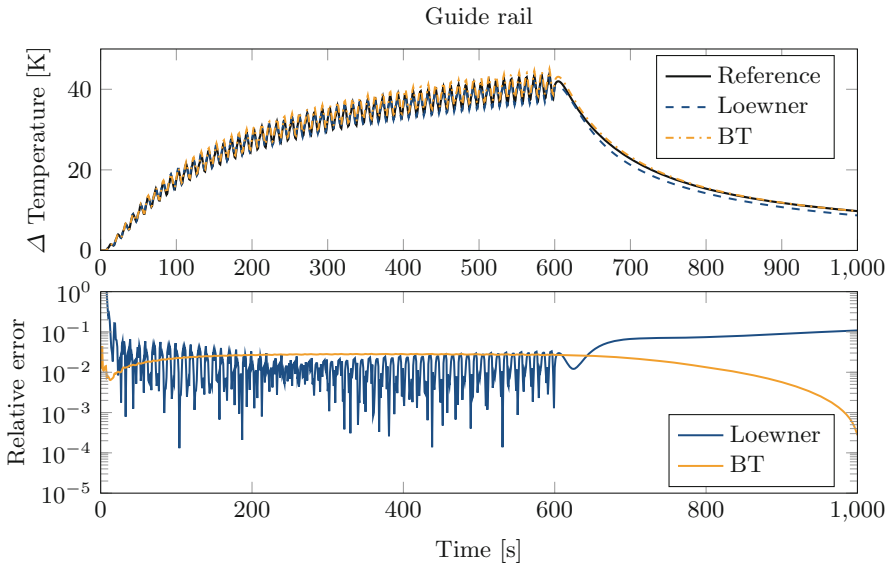


Fig. 5. Temperature change at the midpoint of the upper rail in A1 during the simulated work process. Time responses of the reference full order model and the surrogate models computed by the Loewner framework and balanced truncation as well as the corresponding relative errors.

As expected, the accuracy of the reduced-order model computed with balanced truncation is better over nearly the complete time range for both evaluation points.

5 Conclusion

In this contribution, we showed and compared two methods to compute compact surrogate models describing the thermal behavior of machine tools. The time-varying heat flows between subassemblies resulting from relative movements of the machine were modeled using a weighted average on the interaction surfaces. The coupling was preserved in the reduced space and the reduction processes of different subassemblies were therefore independent of each other. This theoretically also allows the reduction of the subassemblies using different reduction methods, e.g., based on model properties like local nonlinearities [19]. The relatively high number of inputs and outputs did not pose problems to the reduction algorithms.

We compared reduced-order models computed with balanced truncation, an intrusive MOR method, to surrogates obtained from the non-intrusive Loewner framework. While the reduced-order models computed with balanced truncation were more accurate, the Loewner framework does not require access to the assembled system matrices of the full order model and is, therefore, especially suited for an industrial setting.

Acknowledgment. Funded by the German Research Foundation – Project-ID 174223256 – TRR 96.

References

1. Antoulas, A.C.: Approximation of Large-Scale Dynamical Systems. Adv. Des. Control, vol. 6. SIAM Publications, Philadelphia (2005). <https://doi.org/10.1137/1.9780898718713>
2. Antoulas, A.C., Beattie, C., Gugercin, S.: Interpolatory Methods for Model Reduction. Computational Science and Engineering, vol. 21. SIAM Publications, Philadelphia (2020). <https://doi.org/10.1137/1.9781611976083>
3. Antoulas, A.C., Lefteriu, S., Ionita, A.C.: A tutorial introduction to the Loewner framework for model reduction. In: Benner, P., Ohlberger, M., Cohen, A., Willcox, K. (eds.) Model Reduction and Approximation, pp. 335–376. SIAM, Philadelphia (2017). <https://doi.org/10.1137/1.9781611974829.ch8>
4. Benner, P.: Numerical linear algebra for model reduction in control and simulation. GAMM-Mitt. **29**(2), 275–296 (2006). <https://doi.org/10.1002/gamm.201490034>
5. Benner, P., Bonin, T., Faßbender, H., Saak, J., Soppa, A., Zaeh, M.: Novel model reduction techniques for control of machine tools. In: Proceedings of ANSYS Conference & 27. CADFEM Users’ Meeting 2009, 18–20 November 2009, Congress Center Leipzig. CADFEM GmbH, Grafing (2009). ISBN/ISSN 3-937523-06-5
6. Benner, P., Saak, J.: Numerical solution of large and sparse continuous time algebraic matrix Riccati and Lyapunov equations: a state of the art survey. GAMM-Mitt. **36**(1), 32–52 (2013). <https://doi.org/10.1002/gamm.201310003>

7. Benner, P., Werner, S.W.R.: MORLAB—the Model Order Reduction LABORatory. In: Benner, P., Breiten, T., Faßbender, H., Hinze, M., Stykel, T., Zimmermann, R. (eds.) *Model Reduction of Complex Dynamical Systems*. ISNM, vol. 171, pp. 393–415. Springer, Cham (2021). https://doi.org/10.1007/978-3-030-72983-7_19
8. Bonin, T., Soppa, A., Saak, J., Zäh, M., Faßbender, H., Benner, P.: Moderne Modellordnungsreduktionsverfahren für Finite-Elemente-Modelle zur Simulation von Werkzeugmaschinen. In: *Fachtagung MECHATRONIK 2011*, Dresden, pp. 333–338 (2011)
9. Gosea, I.V., Poussot-Vassal, C., Antoulas, A.C.: On enforcing stability for data-driven reduced-order models. In: *2021 29th Mediterranean Conference on Control and Automation (MED)*. IEEE (2021). <https://doi.org/10.1109/med51440.2021.9480216>
10. Hernández-Becerro, P.: Efficient thermal error models of machine tools. Ph.D. thesis, ETH Zurich (2020). <https://doi.org/10.3929/ETHZ-B-000449279>
11. Hernández-Becerro, P., Spescha, D., Wegener, K.: Model order reduction of thermo-mechanical models with parametric convective boundary conditions: focus on machine tools. *Comput. Mech.* **67**(1), 167–184 (2020). <https://doi.org/10.1007/s00466-020-01926-x>
12. Jones, D., Snider, C., Nassehi, A., Yon, J., Hicks, B.: Characterising the digital twin: a systematic literature review. *CIRP J. Manuf. Sci. Technol.* **29**, 36–52 (2020). <https://doi.org/10.1016/j.cirpj.2020.02.002>
13. Köhler, M.: On the closest stable descriptor system in the respective spaces RH_2 and RH_∞ . *Linear Algebra Appl.* **443**, 34–49 (2014). <https://doi.org/10.1016/j.laa.2013.11.012>
14. Lang, N., Saak, J., Benner, P.: Model order reduction for systems with moving loads. *at-Automatisierungstechnik* **62**(7), 512–522 (2014). <https://doi.org/10.1515/auto-2014-1095>
15. Mayo, A.J., Antoulas, A.C.: A framework for the solution of the generalized realization problem. *Linear Algebra Appl.* **425**(2–3), 634–662 (2007). <https://doi.org/10.1016/j.laa.2007.03.008>
16. Saak, J., Siebelts, D., Werner, S.W.R.: A comparison of second-order model order reduction methods for an artificial fishtail. *at-Automatisierungstechnik* **67**(8), 648–667 (2019). <https://doi.org/10.1515/auto-2019-0027>
17. Sauerzapf, S., Vettermann, J., Naumann, A., Saak, J., Beiteltschmidt, M., Benner, P.: Simulation of the thermal behavior of machine tools for efficient machine development and online correction of the tool center point (TCP)-displacement. In: *Special Interest Group Meeting on Thermal Issues Laboratory for Machine Tools and Production Engineering (WZL) of RWTH Aachen, Germany*, February 2020. EUSPEN (2020)
18. Vettermann, J., et al.: Model order reduction methods for coupled machine tool models. *MM Sci. J.* **2021**(3), 4652–4659 (2021). <https://doi.org/10.17973/mmsj.2021.7.2021072>
19. Vettermann, J., Steinert, A., Brecher, C., Benner, P., Saak, J.: Compact thermo-mechanical models for the fast simulation of machine tools with nonlinear component behavior. *at-Automatisierungstechnik* **70**(8), 692–704 (2022). <https://doi.org/10.1515/auto-2022-0029>

Open Access This chapter is licensed under the terms of the Creative Commons Attribution 4.0 International License (<http://creativecommons.org/licenses/by/4.0/>), which permits use, sharing, adaptation, distribution and reproduction in any medium or format, as long as you give appropriate credit to the original author(s) and the source, provide a link to the Creative Commons license and indicate if changes were made.

The images or other third party material in this chapter are included in the chapter's Creative Commons license, unless indicated otherwise in a credit line to the material. If material is not included in the chapter's Creative Commons license and your intended use is not permitted by statutory regulation or exceeds the permitted use, you will need to obtain permission directly from the copyright holder.

